ISSN 1062-8738, Bulletin of the Russian Academy of Sciences. Physics, 2013, Vol. 77, No. 2, pp. 217–220. © Allerton Press, Inc., 2013.
Original Russian Text © V.A. Pustovarov, A.N. Razumov, V.Yu. Ivanov, D.I. Vyprintsev, N.G. Shvalev, 2013, published in Izvestiya Rossiiskoi Akademii Nauk. Seriya Fizicheskaya, 2013, Vol. 77, No. 2, pp. 240–243.

Time-Resolved Luminescence of $LaBr_3$–Ce Scintillation Crystals Upon Selective UV–VUV–XUV Excitation

V. A. Pustovarov[a], A. N. Razumov[a], V. Yu. Ivanov[a], D. I. Vyprintsev[b], and N. G. Shvalev[b]

[a] *Yeltsin Ural Federal University, Yekaterinburg, 620002 Russia*
[b] *STARK Company, Obninsk, Kaluga oblast, 249035 Russia*
e-mail: razumov-a@prosoftsystems.ru

Abstract—The time-resolved photoluminescence (PL) of $LaBr_3$–Ce scintillation spectrometric crystals produced in Russia is measured upon excitation using synchrotron radiation with photon energies of 3.7–21 and 45–290 eV at temperatures of 295 and 7.5 K. The PL spectra and decay curves are measured for excitation in the transparency range, at the edge of fundamental absorption, at the interband transitions, and in the range of inner-shell absorption. It is demonstrated that the PL yield is not proportional to the excitation energy, and that the PL decay curves are modified in the range of photoionization of the 3*d* (Br) and 4*d* (La) inner shells and, especially, in the range of giant resonance.

DOI: 10.3103/S1062873813020287

INTRODUCTION

$LaBr_3$–Ce crystals are state-of-the-art scintillation materials for spectrometric detectors of photon radiation. Crystals from Saint-Gobain are characterized by relatively high photon yields (~60000 photons/MeV), relatively fast decay of scintillation pulses ($\tau < 25$ ns), and high stability of parameters over a wide range of temperatures. The crystals can be used in spectrometry and various medical applications due to their relatively high energy resolution and radiation hardness [1–3]. At present, the main problem is studying the energy nonproportionality of the photon yield, especially in the X-ray spectral range. Such a dependence was studied in [4] using synchrotron radiation (SR) in the X-ray range of 1.4 to 100 keV. The $d \rightarrow f$ luminescence of the Ce^{3+} ions in $LaBr_3$–Ce upon ultraviolet (UV) and vacuum ultraviolet (VUV) excitation was studied in [5], in which the edge of fundamental absorption and the energy of interband transitions ($E_g = 5.9$ eV at $T = 10$ K) were determined.

In this work, we study the photoluminescence (PL) of $LaBr_3$–Ce crystals at temperatures of 295 and 7.5 K upon the UV and VUV excitation and excitation in the ultrasoft X-ray range (extreme UV range (XUV)) of 45 to 290 eV that spans the photoionization potentials of several inner shells. The aim of this work was to analyze the radiative relaxation processes in $LaBr_3$–Ce crystals for the PL over a wide range of energies.

EXPERIMENTAL

Optical-quality single crystals from STARK Company were grown using the Bridgeman method in quartz ampoules at a rate of 1 mm/h and were certified via X-ray diffraction and chemical analysis [6]. In our experiments, we used $LaBr_3$–Ce crystals (5 wt % Ce^{3+}) freshly cleaved in dry air with dimensions of $10 \times 8 \times 1$ mm. The crystals were hygroscopic and the time interval between cleavage and the placing of crystal in the ultra-high-vacuum cryostat with a residual working pressure of $\sim 2 \times 10^{-7}$ Pa was no greater than one minute.

In our experiments, we employed time-resolved luminescence spectroscopy on the SR channels at the HASYLAB laboratory (DESY, Hamburg): channel I (Superlumi station, UV/VUV range) and channel BW3 (XUV range). Upon UV/VUV excitation, we measured the PL spectra using an ARC Spectra Pro-308 0.3-m-base monochromator and a Hamamatsu R6358P PMT. The measurements of the time-integrated PL spectra were supplemented with measurements of the PL spectra in two time windows with width Δt that were delayed relative to the SR excitation pulse by δt. The parameters of the time gating were $\delta t_1 = 1.4$ ns and $\Delta t_1 = 14$ ns (fast component) and $\delta t_2 = 52$ ns and $\Delta t_2 = 20$ ns (slow component). The time resolution of the detection system was no greater than 0.8 ns, and the time interval between the SR pulses was 96 ns. The PL excitation spectra were normalized by a number of photons equal to that of those incident on the sample using sodium salicylate. A description of the equipment and experimental procedure for conducting measurements on the BW3 channel in the XUV range can be found in [7]. The spectral resolution was 0.1 eV at 100 eV.

RESULTS AND DISCUSSION

Figures 1–3 present the main experimental results. At room temperature, the PL spectrum was a nonele-

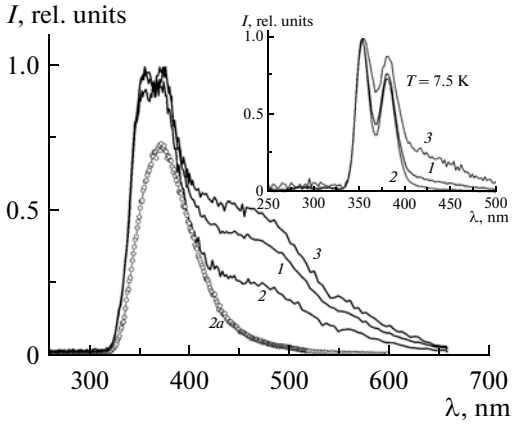

Fig. 1. Time-resolved PL spectra of $LaBr_3$–Ce at E_{exc} = 6.88 eV and T = (*1*)–(*3*) 7.5 and (*2a*) 295 K: (*1*) time-integrated spectrum, (*2*) and (*2a*) fast component, and (*3*) slow component.

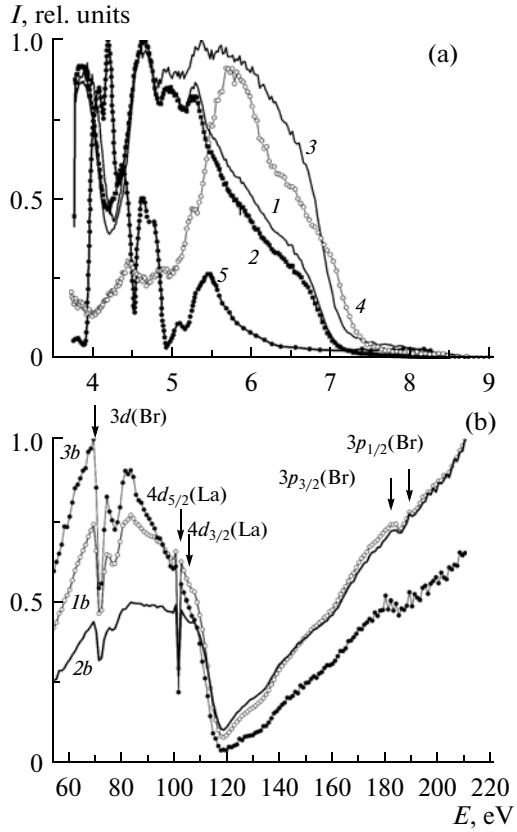

Fig. 2. Time-resolved PL excitation spectra of $LaBr_3$–Ce at λ_{rad} = 356 nm and T = (*1*)–(*3*) and (*1b*)–(*3b*) 295 and (*4*) and (*5*) 10 K: (*1*), (*1b*), and (*5*) time-integrated spectra; (*2*), (*2b*), and (*4*) fast component; and (*3*) and (*3b*) slow component. Spectrum *5* is the result from [5] for $LaBr_3$–Ce (0.5 wt %). The arrows indicate the photoionization energies of inner shells.

mentary band formed by typical $d \rightarrow f$ radiative transitions from the excited state to the ground state ($F_{5/2}$, $F_{7/2}$) of the Ce^{3+} ions and split by the crystal field (Fig. 1). Such splitting is clearly seen at lower temperatures at any (UV/VUV/XUV) excitation. Our time-resolved experiments revealed the long-wavelength shift of the spectrum of the slow component. This was due to the PL decay kinetics at fixed excitation energy E_{exc} depending on radiation wavelength λ_{rad}. Figure 3 shows the PL decay curves at T = 295 K for two values of λ_{rad}. For λ_{rad} = 430 nm, the decay curve exhibits a developed slow component of the microsecond range that forms the pedestal of the PL decay curve. The shift of the PL spectrum of the slow component is clearly seen at low temperature (inset to Fig. 1). To find the reasons for modification of the PL spectral shapes in the time-resolved experiments, we measured the PL spectra of a freshly cleaved crystal, which was kept in a cryostat at a residual pressure of ~1 Pa for one day. A broad long-wavelength band emerged in the PL spectrum in the interval 430–460 nm, and the intensity of this band increases at low temperature. This indicates a possible relationship between this PL band and the low-temperature emissions of corrosion products that result from the interaction of hygroscopic crystals in a forevacuum with residual atmospheric gases. The PL spectrum's shape and the wavelength dependence of the PL decay kinetics could nevertheless be related to the effect of the point defects in a crystalline structure, or to the microscopic defects that form in the course of crystal growth, particularly the effect of the phase of lanthanum oxybromide, the presence of which is possible in the bulk of the crystal under the above growth conditions [8].

Note the complicated shape of the PL excitation spectra and considerable difference between the time-integrated spectrum and the time-resolved spectrum. Figure 2 shows the spectra for the UV–VUV and XUV spectral ranges separately.

In the low-energy interval from 3.7 to 5.0 eV, the bands in the PL excitation spectrum are determined by the $f \rightarrow d$ intracenter transitions in the Ce^{3+} ion. We observe a monoexponential decay (Fig. 3a, table), but the decay time depends on the excitation energy. At E_{exc} = 4.27 eV (the energy that corresponds to the minimum on the PL excitation spectrum), the decay time is reduced. Faster decay of the intracenter PL was observed for several crystals doped with Ce^{3+} [9], and hence can be related to electronic transitions in the Ce^{3+} ions located in the vicinity of the defects of crystal structure in $LaBr_3$–Ce. When E_{exc} is greater than 5 eV, we observe the nonexponential decay of the $d \rightarrow f$ luminescence of Ce^{3+} ions with microsecond components. This is clearly seen in the time-resolved PL spectra (curves *2* and *3* in Fig. 2a). Decay curve $I(t)$ is well approximated using two exponential functions:

$$I(t) = A_1\exp[-(t - t_0)/\tau_1] + A_2\exp[-(t - t_0)/\tau_2] + I_0,$$

where parameter I_0 considers the contribution from the slow microsecond components. Table shows the

parameters of the PL decay curves at several typical values of E_{exc}. In accordance with the estimates from [5], the minimum energy of the interband transitions in $LaBr_3$ is $E_g = 5.9$ eV at $T = 10$ K. Our estimate is based on an analysis of the PL excitation spectrum (curve *5* in Fig. 2a). However, we obtained substantially different results (compare spectra *4* and *5*, measured at $T = 10$ K). In the crystals under study, the PL yield drops sharply only at energies greater than 6.6 eV. Therefore, energy E_g is estimated to be 7.0–7.2 eV. Such a difference in the PL excitation spectra cannot be due only to the difference between the Ce^{3+} ion concentrations. We assume that the reason lies in the difference between the concentrations of point or macroscopic defects of the crystalline structures in the investigated crystals provided by different manufacturers. Additional independent procedures are needed for a correct estimate of energy E_g in $LaBr_3$.

Upon excitation in the range of fundamental absorption ($E_{exc} > 7.2$ eV), the PL yield falls to almost zero, testifying to the relatively high mobility of band electrons and holes and their nonradiative recombination on the surface. In the VUV range, we do not observe an increase in the PL yield up to an energy of 21 eV (not shown on the spectra). The effect of the multiplication of electronic excitations, inherent in any effective scintillation process, is thus not observed in this energy range. However, the effect is clearly seen at high energies in the XUV range (Fig. 2b). For *p*-type crystals with relatively narrow valence bands, the threshold energy of the effect ranges from $2E_g$ to $3E_g$. We therefore assume that energy $E_g = 5.9$ eV was substantially underestimated in [5].

In the XUV range, we observe a monotonic increase in the PL yield with an increase in excitation energy E_{exc}, along with narrow dips and a broad deep minimum at 118 eV. The energies of narrow dips correspond to the known photoionization potentials of inner shells (the energies and corresponding electronic states are marked with arrows). Specific features are observed in the photoionization range of the 3*d* (Br) and 4*d* (La) states. Specific features of the PL excitation spectra are less developed in the excitation range of the deeper 3*p* states (Br). The excitation of scintillations in these crystals was analyzed in [1, 2, 5]. The excitation results from subsequent electron–hole radiative recombination on the Ce^{3+} centers. The narrow dips on the PL excitation spectrum must therefore be related to the transition of electrons from the ground levels to the conduction band. The broad deep minimum at 118 eV in the PL excitation spectrum correlates with the absorption spectrum of the lanthanum film [10]: the spectra are completely antibatic. The absorption of lanthanides in this energy range is considered a manifestation of giant resonance [11]. In this range of fundamental absorption, the absorption coefficient is extremely high (~10^5–10^6 cm^{-1}) and the absorption of photons with such energies takes place only in a very thin surface layer of the crystal. An increase in the absorption coefficient in the range of photoionization potentials and giant resonance stimulates the nonradiative recombination of charge carriers on the surface. The competition between the

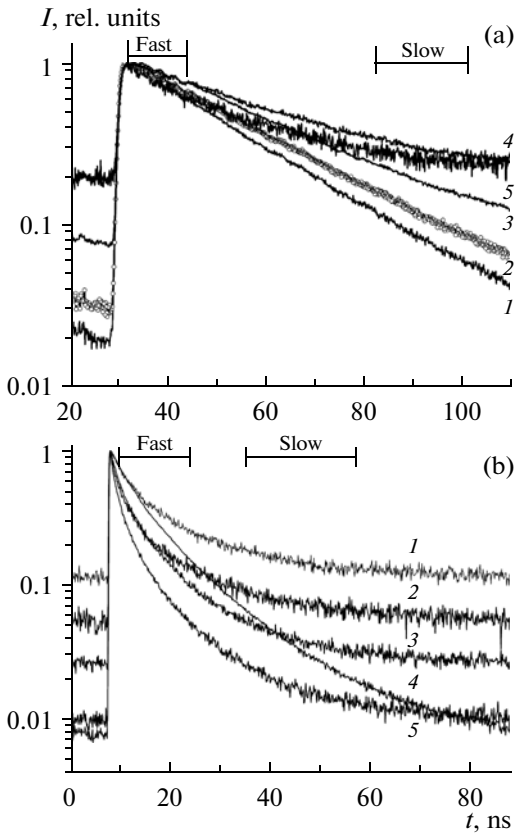

Fig. 3. PL decay curves of $LaBr_3$–Ce for the PL excitation in (a) UV–VUV and (b) XUV spectral ranges at $T = 295$ K: (a) $\lambda_{rad} = 356$ nm and $E_{exc} = (1)$ 4.27, 3.87, 4.6, (*2*) 4.86, (*3*) 5.52, (*4*) 6.88, and (*5*) 7.75 eV and (b) $\lambda_{rad} = (1)$ and (*2*) 430 and (*3*)–(*5*) 356 nm and $E_{exc} = (1)$ and (*3*) 130, (*2*) and (*5*) 118, and (*4*) 500 eV. Segments Fast and Slow show the time windows that correspond to the fast and slow components, respectively, in the time-resolved experiments.

Parameters of the $LaBr_3$–Ce PL decay curves

E_{exc}, eV	$\lambda_{rad} = 356$ nm			$\lambda_{rad} = 430$ nm		
	τ_1, ns	τ_2, ns	I_0	τ_1, ns	τ_2, ns	I_0
	$T = 295$ K					
3.9; 4.6; 4.9	25.4	–	0.03	33	–	0.08
4.27	23	–	0.015	26.5	–	0.03
7.75	15	32	0.2			
118	1.3	8	0.01	2.9	15.0	0.06
130	2.1	10.2	0.03	3	14.2	0.11
500	5.9	16	0.01			
	$T = 7.5$ K					
95	1.9	10.5	0.032			
102	1.1	9.8	0.021	13.3	126	0.21
119	1.0	9.2	0.022			
286	2.2	12.8	0.04			

radiative recombination of charge carriers on the Ce^{3+} centers and the nonradiative recombination on the surface accounts for the structure of the PL excitation spectrum.

The nonexponential PL decay curve depends considerably on E_{exc} (Fig. 3). Decay times τ_1 and τ_2 diminish when the excitation photon energies correspond to narrow dips and the range of giant resonance in the PL excitation spectrum (the calculation error was no greater than 5%). This result is also related to the competition between the radiative recombination of band carriers on the Ce^{3+} centers and the nonradiative energy loss in a thin surface layer.

The PL spectral features at temperature $T = 7.5$ K are similar to the spectral features at room temperature. In the excitation range of the 3*s*, 3*p* (Br), 4*s*, and 4*p* (La) deep inner shells (up to 209 eV), the structure in the PL excitation spectrum is negligible (as at the temperature $T = 295$ K). The time-resolved spectra differ because the PL decay kinetics also depends on energy E_{exc}. In the range of the dips and giant resonance, the PL decay times diminish. Note that the contribution from the slow (microsecond) components is no greater than 2–4% of the peak intensity for $\lambda_{rad} = 356$ nm at $T = 7.5$ K. This data and the negligible temperature dependence of the luminescence yield in the interval 90–400 K [3] indicate that $LaBr_3$–Ce can be used as a fast scintillator over a wide range of temperatures.

ACKNOWLEDGMENTS

This work was supported by the HASYLAB DESY (Deutsches Elektronen Synchrotron, Hamburg, Germany), project nos. I-20110050 and II-20080119EC.

REFERENCES

1. van Loef, E.V.D., Dorenbos, P., van Ejik, C.W.E., et al., *Appl. Phys. Lett.*, 2001, vol. 79, p. 1573.
2. Shah, K.S., Glodo, J., Klugerman, M., et al., *IEEE Trans. Nucl. Sci.*, 2003, vol. 50, p. 2410.
3. www.detectors.saint-gobain.com/Brillance380.aspx
4. Khodyuk, I.V. and Dorenbos, P., *J. Phys.: Condens. Matter*, 2010, vol. 22, p. 485402.
5. Dorenbos, P., van Loef, E.V.D., Vink, A.P., et al., *J. Lumin.*, 2006, vol. 117, p. 147.
6. Vyprintsev, D.I. and Novoselov, I.I., in *Tez. dokl. XII Nats. konf. po rostu kristallov. 23-27 oktyabrya 2006 g* (Proc. 12th National Conf. on Crystal Growth, Oct. 23–27, 2006), Moscow: Institut kristallografii RAN, p. 283.
7. Pustovarov, V.A., Ivanov, V.Yu., Vyprintsev, D.I., and Shvalev, N.G., *Pis'ma Zh. Tekh. Fiz.,* 2012, vol. 38, no. 17, p. 15.
8. Yang, P. and Wang, J., *J. Mater. Sci. Technol.,* 2009, vol. 25, no. 6, p. 753.
9. Omelkov, S.I., Brik, M.G., Kirm, M., Pustovarov, V.A., et al., *J. Phys. Condens. Matter*, 2011, vol. 23, p. 105501.
10. Shulakov, A.S., Stepanov, A.P., and Braiko, A.P., *Fiz. Tverd. Tela*, 1992, vol. 34, no. 8, p. 2445.
11. Zimkina, T.M., Fomichev, V.A., Gribovskii, S.A., and Zhukova, I.I., *Fiz. Tverd. Tela*, 1967, vol. 9, no. 5, p. 1447.